

LUMINOSITY FUNCTIONS OF LMXBS IN CENTAURUS A: GLOBULAR CLUSTERS VERSUS THE FIELD

RASMUS VOSS^{1,2}, MARAT GILFANOV^{3,4}, GREGORY R. SIVAKOFF^{5,8}, RALPH P. KRAFT⁶, ANDRÉS JORDÁN^{6,7}, SOMAK RAYCHAUDHURY⁹, MARK BIRKINSHAW¹⁰, NICOLA J. BRASSINGTON⁶, JUDITH H. CROSTON¹¹, DANIEL A. EVANS^{12,6}, WILLIAM R. FORMAN¹³, MARTIN J. HARDCASTLE¹¹, WILLIAM E. HARRIS¹⁴, CHRISTINE JONES¹³, ADRIENNE M. JUETT¹⁵, STEPHEN S. MURRAY⁶, CRAIG L. SARAZIN⁵, KRISTIN A. WOODLEY¹⁶, AND DIANA M. WORRALL¹⁰

Draft version November 15, 2018

ABSTRACT

We study the X-ray luminosity function (XLF) of low mass X-ray binaries (LMXB) in the nearby early-type galaxy Centaurus A, concentrating primarily on two aspects of binary populations: the XLF behavior at the low luminosity limit and comparison between globular cluster and field sources. The 800 ksec exposure of the deep *Chandra* VLP program allows us to reach a limiting luminosity of $\sim 8 \cdot 10^{35}$ erg s⁻¹, about $\sim 2 - 3$ times deeper than previous investigations. We confirm the presence of the low luminosity break in the overall LMXB XLF at $\log(L_X) \approx 37.2 - 37.6$ below which the luminosity distribution follows a $dN/d(\ln L) \sim \text{const}$ law. Separating globular cluster and field sources, we find a statistically significant difference between the two luminosity distributions with a relative underabundance of faint sources in the globular cluster population. This demonstrates that the samples are drawn from distinct parent populations and may disprove the hypothesis that the entire LMXB population in early type galaxies is created dynamically in globular clusters. As a plausible explanation for this difference in the XLFs, we suggest that there is an enhanced fraction of helium accreting systems in globular clusters, which are created in collisions between red giants and neutron stars. Due to the 4 times higher ionization temperature of He, such systems are subject to accretion disk instabilities at ≈ 20 times higher mass accretion rate, and therefore are not observed as persistent sources at low luminosities.

Subject headings: galaxies: individual: Centaurus A – X-rays: binaries – X-rays: galaxies

1. INTRODUCTION

Electronic address: rvoss@mpe.mpg.de

¹ Max-Planck-Institut für extraterrestrische Physik, Giessenbachstrasse, D-85748, Garching, Germany

² Excellence Cluster Universe, Technische Universität München, Boltzmannstr. 2, D-85748, Garching, Germany

³ Max Planck Institut für Astrophysik, Karl-Schwarzschild-Str. 1, D-85741, Garching, Germany

⁴ Space Research Institute, Russian Academy of Sciences, Profsoyuznaya 84/32, 117997 Moscow, Russia

⁵ Department of Astronomy, University of Virginia, P.O. Box 400325, Charlottesville, VA 22904-4325

⁶ Harvard-Smithsonian Center for Astrophysics, 60 Garden Street, MS-67, Cambridge, MA 02138

⁷ Departamento de Astronomía y Astrofísica, Pontificia Universidad Católica de Chile, Casilla 306, Santiago 22, Chile

⁸ Department of Astronomy, 4055 McPherson Laboratory, Ohio State University, 140 West 18th Avenue, Columbus, OH 43210-1173

⁹ School of Physics and Astronomy, University of Birmingham, Edgbaston, Birmingham B15 2TT, UK

¹⁰ Department of Physics, University of Bristol, Tyndall Avenue, Bristol BS8 1TL, UK

¹¹ School of Physics, Astronomy and Mathematics, University of Hertfordshire, College Lane, Hatfield, Hertfordshire AL10 9AB, UK

¹² MIT Kavli Institute, 77 Massachusetts Avenue, Cambridge, MA 02139

¹³ Smithsonian Astrophysical Observatory, Harvard-Smithsonian Center for Astrophysics, Cambridge, MA 02138

¹⁴ Department of Physics and Astronomy, McMaster University, Hamilton, ON L8S 4M1

¹⁵ NASA Postdoctoral Fellow, Laboratory for X-ray Astrophysics, NASA Goddard Space Flight Center, Greenbelt, MD 20771

¹⁶ Department of Physics and Astronomy, McMaster University, Hamilton, ON L8S 4M1

With the advent of *Chandra*, the study of populations of X-ray binaries in nearby galaxies became possible (e.g. Sarazin et al. 2000; Kraft et al. 2001; Kundu et al. 2002). In young stellar populations the high mass X-ray binaries dominate, and the luminosity function (LF) was found to be a simple power law $dN/dL_X \propto L_X^{-\Gamma}$ with a differential slope of $\Gamma \sim 1.6$ (Grimm et al. 2003), with an indication of flattening at very low luminosities $\lesssim \log(L_X) = 35.5$, probably due to the propeller effect¹⁷ (Shtykovskiy & Gilfanov 2005). The LF in old stellar populations is dominated by low mass X-ray binaries (LMXBs) and was shown to be steep at the bright end, $\log(L_X) > 37.5$, with a power law index in the $\sim 1.8 - 2.5$ range (Gilfanov 2004; Kim & Fabbiano 2004), flattening to $dN/dL \propto L^{-1}$ below $\log(L_X) \lesssim 37.5$ (Gilfanov 2004; Voss & Gilfanov 2007a). While the low luminosity break is observed in the bulges of spiral galaxies, there is no consensus on the shape below $\sim 10^{37}$ erg s⁻¹ in elliptical galaxies (Voss & Gilfanov 2006; Kim et al. 2006). Currently the only elliptical galaxy in which it is possible to observe X-ray sources well below 10^{37} erg s⁻¹ is Centaurus A (Cen A).

The number of LMXBs per unit stellar mass is known to be \sim two orders of magnitude higher in Galactic globular clusters (GCs) than in the field of the Milky Way (Clark 1975). Also in external galaxies, the frequency of LMXBs is particularly high in GCs (e.g.

¹⁷ At low mass accretion rates the centrifugal barrier imposed by the magnetosphere of the spinning neutron star may inhibit the flow of matter towards the neutron star, thus quenching the X-ray emission (Illiaronov & Sunyaev 1975).

Sarazin et al. 2003; Minniti et al. 2004; Jordán et al. 2007; Posson-Brown et al. 2009), and this is attributed to dynamical processes in which LMXBs are formed in close stellar encounters. The same mechanisms also have been shown to be responsible for the formation of a significant number of "surplus" LMXBs in the dense inner bulge of M 31 (Voss & Gilfanov 2007b). It is currently a subject of debate whether the entire LMXB population in (early type) galaxies was formed in GCs (White et al. 2002; Kundu et al. 2002; Maccarone 2003; Juett 2005; Irwin 2005; Humphrey & Buote 2006; Kundu et al. 2007). This suggestion has been confronted by the statistics of LMXBs and globular clusters in spiral galaxies and especially in the Milky Way. Also, evidence has been found that the luminosity distributions of LMXBs in globular clusters (and in the central parts of M 31) and in the field differ at the low luminosity end, below $\sim 10^{37}$ erg s $^{-1}$, (Voss & Gilfanov 2007a; Fabbiano et al. 2007; Woodley et al. 2008; Kim et al. 2009), which would be a strong indication of different formation histories.

Cen A is one of the best available candidates for the study of the LF of LMXBs in an early-type galaxy, as it is massive enough to contain a sufficient number of LMXBs and is sufficiently nearby that a meaningful sensitivity can be achieved in a reasonable exposure time with *Chandra*. Previous studies of Cen A with *Chandra* have yielded information on the nucleus (Evans et al. 2004), the interstellar medium (Kraft et al. 2003, 2007, 2008; Croston et al. 2009), the jet (Kraft et al. 2002; Hardcastle et al. 2003, 2007; Worrall et al. 2008), and the shell structures (Karovska et al. 2002). The off-center population of point sources was first studied by Kraft et al. (2001). Minniti et al. (2004) investigated optical counterparts of X-ray sources, and the luminosity function and spatial distribution of the LMXBs were investigated by Voss & Gilfanov (2006). Jordán et al. (2008) and Woodley et al. (2008) studied the connection between GCs and LMXBs, and Sivakoff et al. (2008a) studied a transient black hole candidate.

Recently, Cen A has been the target of a *Chandra* VLP program, which brought the total exposure time to ~ 800 ks. With this exposure, individual point sources can be detected down to the luminosity of $\sim 6 \cdot 10^{35}$ erg/sec and the population of compact sources as a whole can be studied in a statistically complete manner down to $\sim 8 \cdot 10^{35}$ erg/s. The significant, about 4-fold, increase in the exposure is advantageous for the study of the astrophysics of compact sources. The results of the detailed analysis of these data including the source lists will be published in forthcoming papers. In this paper we take advantage of the increased *Chandra* exposure to perform a deeper study of the luminosity distribution of LMXBs, with the main focus on the XLF behavior in the low luminosity regime and the difference between the LFs of the field and globular cluster LMXBs.

2. DATA ANALYSIS

We combined all the available *Chandra* ACIS observations of Cen A, to obtain the deepest possible combined image. With the high number of point sources, it was possible to align the individual images to a relative precision of 0.1 arcsec. The individual observations are listed in Table 1, and the data preparation will be described

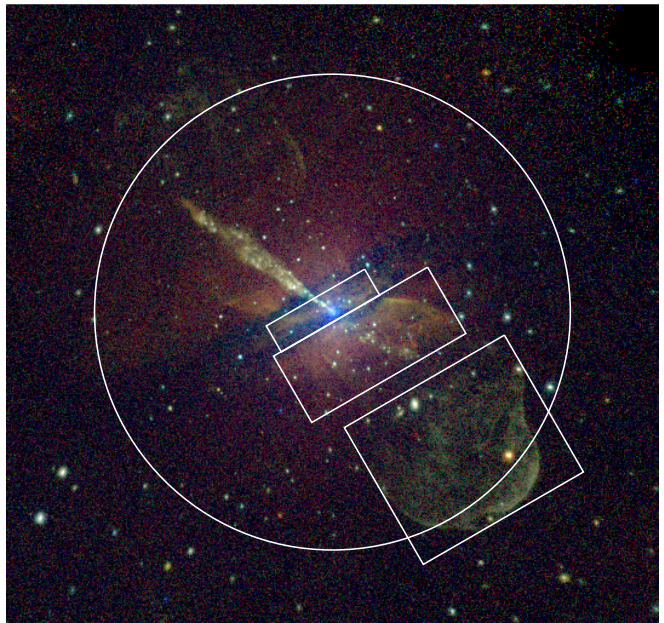


FIG. 1.— The combined X-ray 0.5-8 keV image of Cen A with pixel size 0.492×0.492 arcsec 2 . The region analysed in this paper is inside the circle with a 5 arcmin radius. In the rectangular regions, only sources with a luminosity above 5×10^{36} erg s $^{-1}$ were used, and sources in the jet were excluded. The image was prepared using the data reduction described in the text, including exposure correction and the removal of readout streaks. Besides the large number of X-ray point sources, the jet and the south-west bubble and the absorption lanes are also clearly evident. Traces of a north-west bubble and a counter-jet can also be seen.

in Kraft et al. (in prep). We found that for the point-source detection and luminosity estimation the removal of time intervals with high background was not necessary, as the increased exposure time outweighs the increased background. In each observation readout streaks are seen, due to the luminous central source. To avoid the detection of spurious sources, the streaks were removed from individual images before combining them. As the telescope roll angle varies between the observations, the removed areas are well covered by other observations. The following analyses were done on images filtered to retain only photons in the energy range 0.5-8.0 keV. An exposure map for the combined image was created assuming a power-law spectrum with a photon index of $\Gamma = 1.7$ (while the spectra of individual sources vary, this model provides a good fit to the average spectrum of LMXBs in the *Chandra* band), and Galactic foreground absorption of 8.4×10^{20} cm $^{-2}$ (Dickey & Lockman 1990). The exposure map gives the effective area of the observations at each pixel, taking into account effects such as vignetting, the quantum efficiency degradation of the detectors and the dithering of the telescope. We used CIAO *wavdetect* to detect sources, using the same parameters as in Voss & Gilfanov (2006, 2007a). Compared to the default settings, this ensures that all relevant detection scales are sampled, and the background cleaning is slightly improved.

For each source we estimate the point-spread-function (PSF) by averaging the PSFs of the individual observations, obtained from the *Chandra* PSF library. These were weighted by the values of the exposure maps at the source position, and assuming a constant count rate for a source in all observations. While the sources do vary,

only a few sources are highly variable, and the effect of this on the luminosity function has been found to be small (e.g. Voss & Gilfanov 2006). We compiled a list of all sources within 10 arcmin from the center of Cen A, applying a detection threshold of 10^{-6} (yielding an average of 1 false source per 10^6 0.492×0.492 arcsec² pixels), giving an expectation of approximately 5 spurious detections. In the analysis below we use various subsamples optimized to the specific analyses (e.g. sources in the 7.5-10 arcmin annulus to analyze the background contamination, and sources within the 5 arcmin circle to analyze the LF of field LMXBs). A second sample of sources was compiled, using a detection threshold of 10^{-5} , giving a higher sensitivity at the cost of 10 times more spurious sources.

This list was used for investigating sources coincident with globular clusters (see below). Given the relatively small area covered by each GCs in the image, only 0.25 spurious sources coincident with GCs are expected for this threshold. The count rate was determined using circular apertures with an encircled energy of 85% (radii varying between 1 and 10 arcsec), correcting for contamination from nearby sources, as described in Voss & Gilfanov (2007a). The luminosities of the point sources were then calculated, assuming a power-law spectrum with $\Gamma = 1.7$ and with Galactic foreground absorption, and a distance to Cen A of 3.7 Mpc (Ferrarese et al. 2007).

2.1. Contamination by diffuse emission structures

For the analysis of the population of X-ray point sources, Cen A is in many ways a complicated galaxy. It has a strongly warped dust disc with evidence for star formation. This leads to heavy absorption, and therefore uncertain luminosities, of the X-ray sources in these lanes, as well as a possible contribution to the source sample from high-mass X-ray binaries. The strong emission from the X-ray jet (Kraft et al. 2002; Hardcastle et al. 2007; Worrall et al. 2008) and its structure of many knots make it difficult to detect and identify point sources there. For this reason, all sources in the jet region and within a radius of 20 arcsec from the nucleus were excluded from the following analysis (see Voss & Gilfanov (2006) for exact definition of these regions). In the counter-jet direction, further away from the center of the galaxy, there is a large number of filaments and shell structures (Karovska et al. 2002). These features are all visible in Fig. 1, where the combined X-ray image of Cen A is shown. Many of the features in these regions cannot be clearly distinguished from faint point sources, leading to contamination of the source sample, as illustrated by the Fig.2. The figure shows the LFs of all sources, detected by WAVDETECT task, inside and outside the regions occupied by filaments and shell-like structures (including sources that are obviously part of diffuse structures that are removed from the final sample, see below). The LFs are normalized to the stellar mass and show a higher specific frequency of compact "sources" in the problematic regions, with the contamination increasing severely towards the low luminosity end.

We attempted to clean the point source list, inspecting

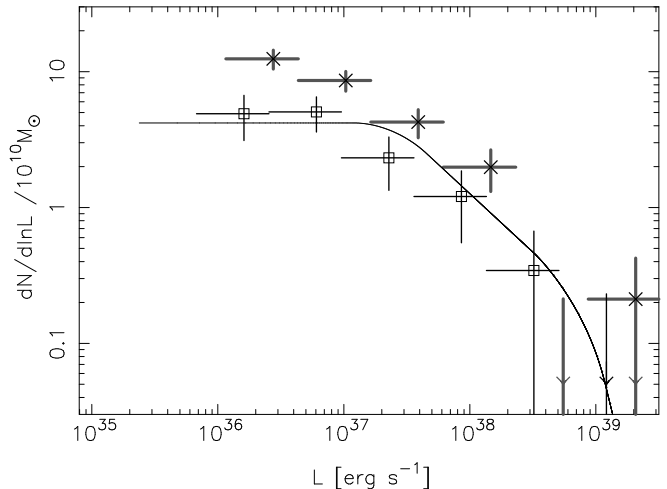


FIG. 2.— Contamination of the luminosity function by structures in the extended emission. The luminosity functions of all compact sources detected by WAVDETECT inside (crosses) and outside (open squares) problematic regions marked by boxes in Fig.1. Only sources within the 5 arcmin circle in Fig.1 were used, and the jet and nucleus regions are excluded in both LFs. The contribution of background sources is subtracted, and LFs are corrected for incompleteness and normalized to the enclosed stellar mass, as discussed in section 3. Above 5×10^{36} erg s⁻¹ structures can be reliably identified and removed.

the image visually and removing all obvious members of extended structures. We found that this procedure works reasonably well for bright sources but fails at the faint end of the luminosity distribution. On the other hand, the problematic regions contain a rather large fraction of the stellar mass, more than a half inside the 5 arcmin area. Given the rather limited number of bright sources in the galaxy, entirely excluding these regions from the analysis would affect notably the statistical quality of the bright end of the luminosity distribution. For this reason we chose to retain relatively bright sources from the problematic regions in the sample, for fluxes above 3.05×10^{-15} erg s⁻¹ cm⁻² ($> 5 \times 10^{36}$ erg s⁻¹ assuming the distance of Cen A). Above this flux it is possible to distinguish between diffuse and point-source emission. Sources that were evidently part of extended structures were identified by eye and removed from the sample. After this removal, 34 sources with luminosities above 5×10^{36} erg s⁻¹ were left in the source list from the contaminated regions. To verify the outcome of this procedure we compared the specific source frequency, per unit stellar mass, in broad luminosity bins, inside and outside the regions dominated by the extended structures and found a good agreement. While we are confident that the majority of false source detections are eliminated by this procedure, a small residual contamination of the sample at the faint end of the luminosity function may still remain. As an additional check, we verified that all results reported below are reproducible with the source lists based on the "good" regions only, albeit with larger errors and/or smaller statistical significance.

Finally, based on the previous X-ray catalogues of the Cen A point sources, we identified 5 sources as foreground stars (see source catalogue of Voss & Gilfanov 2006), and they were also removed from our sample.

2.2. Identification of globular cluster sources

We identified GC counterparts using the catalogues of Woodley et al. (2007) and Jordán et al. (2007, 2008), and a search radius of 2 arcsec. As described above, the X-ray point source list obtained with a relaxed detection threshold of 10^{-5} was used for cross-correlation with the GC catalogs. This gave a total of 49 GC X-ray sources¹⁸ with an expectation of 0.25 false sources (see above) and of 4.25 random coincidences, the latter estimated by displacing the X-ray source list by 5 arcsec in various directions. We did not find additional matches in the catalogues of Harris et al. (2004); Peng et al. (2004). Finally we did not use the catalogue of Minniti et al. (2004). This catalogue was compiled by searching for GCs at the position of X-ray point sources. As the X-ray catalogue used in their study is significantly shallower than ours, it is biased towards bright sources, and such a bias would be problematic for our luminosity function analysis. Inside the search area of the globular clusters, the expected number of background sources is $\lesssim 1$, and therefore most of the random coincidences are with field (non-GC) LMXBs. The catalogue of Jordán et al. (2008) covers 68% of the area investigated in this paper. It is based on *Hubble Space Telescope* images, and is significantly deeper than the catalogue of Woodley et al. (2007), which covers the entire area investigated in this paper. However, of the 40 GC X-ray sources detected inside the area included in the *Hubble Space Telescope* catalogue, only 11 were not found in the catalogue of Woodley et al. (2007). Most of the GCs harboring X-ray sources ($\sim 70\%$) were picked up by the shallower catalogue because the more luminous clusters are more likely to host X-ray sources (e.g. Sarazin et al. 2003; Jordán et al. 2004; Sivakoff et al. 2007). With 7 GCs hosting LMXBs observed outside the area included in the *Hubble Space Telescope* catalogue, we therefore estimate that there may be only ~ 3 undetected GC associated with X-ray sources in our sample. This number is small enough to be neglected.

We note that most of the areas unobserved by the *Hubble Space Telescope* are in regions of relatively low stellar and GC density (along the minor axis of Cen A) and therefore the number of associations between GCs and LMXBs does not scale with the area of the region. 7 X-ray sources match the GC candidates from the catalogue of Minniti et al. (2004), but are not identified as GCs in the analysis of Jordán et al. (2007, 2008). In all these cases we gave preference to the classification based on the *Hubble Space Telescope* data.

3. LUMINOSITY FUNCTIONS

For the analysis of the overall LF of all LMXBs we use the source sample constructed as described in the section 2.1. In order to limit the background-source contamination, we use only sources within 5 arcmin from the center of the galaxy. This area is indicated by the circle in Fig. 1. With the half-light radius of Cen A being ~ 5 arcmin (Dufour et al. 1979), the vast majority of field sources outside this region are background sources (see e.g. the radial source distribution in Fig. 4 of Voss & Gilfanov 2006). Moreover, the incompleteness effects become severe, and the large point spread

¹⁸ The sum of the GC LMXBs in table 2 only add up to 47, as two sources are detected below 10^{36} erg s⁻¹.

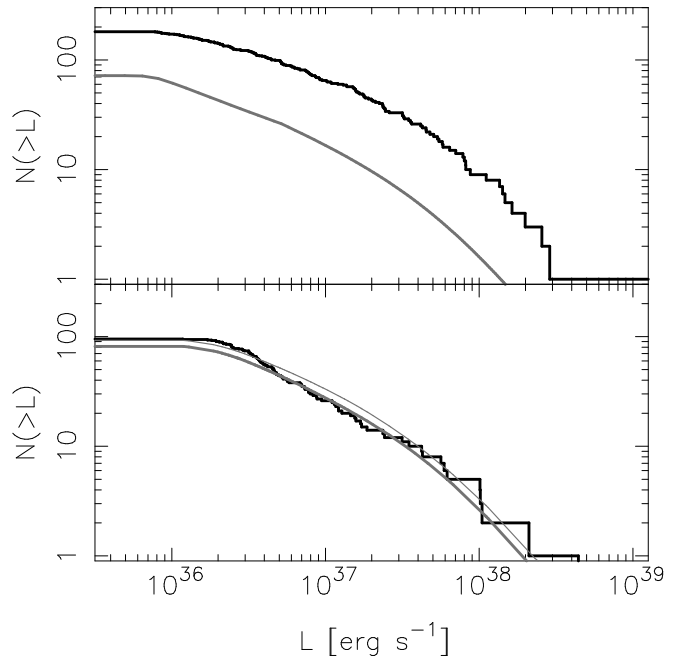


FIG. 3.— Upper panel: the (uncorrected) cumulative source counts within 5 arcmin from the center of Cen A, including both field and GC sources (black), compared to the expected background counts (grey) corrected for incompleteness. The sources belonging to Cen A make up the difference between the curves. Lower panel: the cumulative source counts in the 7.5-10.0 arcmin annulus (black) and the expected background (grey). ~ 10 LMXBs are expected in this annulus in addition to the background sources, and the thin grey line shows the expectation when these are included. The normalization of the background curves is 1.5 times the normalization given by Moretti et al. (2003).

function makes it difficult to distinguish point-like and extended sources. The reduced quality of the LF due to these effects outweighs the small increase in the number of LMXBs. We further construct two sub-samples: the field (non-GC) and the GC sources. The field sources are a selection of non-GC sources from our main sample. In building the sample of GC sources we used the entire galaxy, due to the much reduced probability of contamination by background sources and false sources from sub-structures in the extended emission.

With our selection criteria, the regions used to assemble the field source sample cover about half of the stellar mass of the galaxy at $L_X > 5 \cdot 10^{36}$ erg/s and $\sim 25\%$ at the faint end. In absolute units this corresponds to $6.8 \times 10^{10} M_\odot$ and $3.3 \times 10^{10} M_\odot$ respectively. These numbers were calculated from the K -band light in the *2MASS* Large Galaxy Atlas (Jarret et al. 2003) using $M_*/L_K \simeq 0.76$ (Bell & De Jong 2001) appropriate for the $(B - V) \simeq 0.88$ colour of Cen A. The field sample consists of 154 sources above a flux of 4.3×10^{-16} erg s⁻¹ cm⁻² (\sim the completeness limit, corresponding to a luminosity of $7 \cdot 10^{35}$ erg s⁻¹ at the distance of Cen A), of which ≈ 70 are expected to be background sources, mainly AGN (see below). 34 of these sources come from the problematic regions. The GC sample was constructed using all the data inside $10'$ and contains 47 sources.

The raw LF obtained by binning the sources over luminosity needs to be corrected for incompleteness and contamination from background sources.

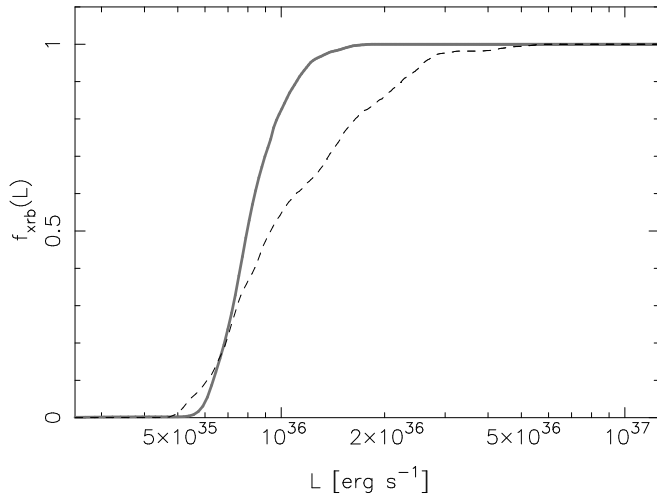


FIG. 4.— The incompleteness function for primordial (non-GC) X-ray binaries within 5 arcmin from the center of Cen A (solid curve) and for the GC sources within 10 arcmin (dashed line).

3.1. Background sources

As in Voss & Gilfanov (2006, 2007a), we used the background source counts from Moretti et al. (2003), converting their soft band results into the full 0.5-8.0 band. Previously (Voss & Gilfanov 2006) we found that the density of resolved CXB sources in the direction towards Cen A was $\sim 50\%$ higher than expected from this calculation, whereas the shape of their $\log N - \log S$ distribution was predicted correctly. Although this excess is larger than the variance in the CXB source density, $\sim 20 - 25\%$, which is typically quoted in the literature, it does not contradict observations of fields where the number of background sources is enhanced due to nearby large-scale structures (Cappelluti et al. 2005; Hudaverdi et al. 2008). Indeed, the Cen A field is located in the direction of the Hydra-Centaurus and Shapley superclusters (Raychaudhury 1989), which may be the main reason for the observed enhancement of the background source density. The relatively low Galactic latitude is also likely to play some role, increasing the number of foreground sources.

We therefore set the normalization of the background $\log N - \log S$ to 1.5 times the nominal value from Moretti et al. (2003). A lower (higher) value of the normalization would cause the observed LF of field sources to become steeper (shallower). In the lower panel of Figure 3 we compare predicted CXB source counts with the observed luminosity distribution of sources detected in the 7.5-10.0 arcmin annulus. In this region the contribution of X-ray binaries located in Cen A is small (~ 10 , estimated from the density of field sources in the inner parts of the galaxy, assuming the density of field LMXBs follow the K -band flux) in comparison with the predicted number of CXB sources (~ 80). The source luminosities were calculated assuming the distance of Cen A; the predicted luminosity distribution for background sources was corrected for incompleteness, as described below. The figure demonstrates good agreement between the two distributions, both in normalization and shape. Indeed a KS-test shows that the observed distribution is compatible (with a KS probability of 70%) with a model consisting of the expected background and 10

LMXBs, which are assumed to follow the LF of Gilfanov (2004). This model is represented by the thin grey line in the lower panel of Figure 3. In agreement with Voss & Gilfanov (2006), we therefore conclude that deviations from the deep-field $\log N - \log S$ must be relatively modest (this was also found for the two regions studied by Hudaverdi et al. 2008). Therefore the possible errors from adopting the background $\log N - \log S$ of Moretti et al. (2003) are smaller than the statistical errors of our sample, and they do not significantly influence our conclusions. We note that the LF of GC sources does not need to be corrected for the contribution of background sources, as the number of such sources coincident with GCs is negligibly small.

The upper panel of Figure 3 shows the cumulative number counts of all sources within 5 arcmin from the center of Cen A, compared to the background expectation. The difference between the two curves arises from sources belonging to Cen A. The vast majority of these sources are LMXBs. Potentially a significant number of HMXBs (~ 30 above our detection limit) could be present in Cen A (Voss & Gilfanov 2006), but most of these are faint and in the very inner part of the galaxy, which is excluded from our analysis, or in the dust lanes, where faint sources are also excluded from our analysis.

3.2. Incompleteness correction

To calculate the completeness of the source samples, we used the method described and tested in Voss & Gilfanov (2006, 2007a). In this method, the incompleteness function at a given luminosity is calculated as the fraction of pixels in which a source with this luminosity would be detected, weighted by the expected spatial distribution of sources. This requires the calculation of the sensitivity for each pixel in the image. To this end, for each of the used `wavdetect` detection scales we computed the threshold sensitivity on a grid of the positions on the image (16 azimuthal angles, 40 radii from the center of Cen A) by inverting the detection method. At each image position the PSF was found and the local background levels were taken from the normalized background maps created by `wavdetect`. The sensitivity for any given position on the image was found from interpolation of the grid values.

For the field sample, the spatial distribution of the LMXBs was assumed to follow the distribution of the K -band light from the 2MASS Large Galaxy Atlas (Jarret et al. 2003) image of Cen A, whereas the distribution of background sources was assumed flat on the scales under consideration. In computing the incompleteness function for the GC sample we assumed equal probability of hosting an LMXB for all of the GCs in our catalogues. This assumption is obviously inaccurate, as more massive/compact GCs are more likely to host LMXBs (e.g. Sarazin et al. 2003; Jordán et al. 2004; Sivakoff et al. 2007). However, if the spatial distribution of GCs does not depend strongly on their structural parameters, this calculation gives a reasonable estimate of the incompleteness function for GC sources. As mentioned above, the background contamination can be neglected for GC sources.

For a given region, the differential LF dN_{xrb}/dL of

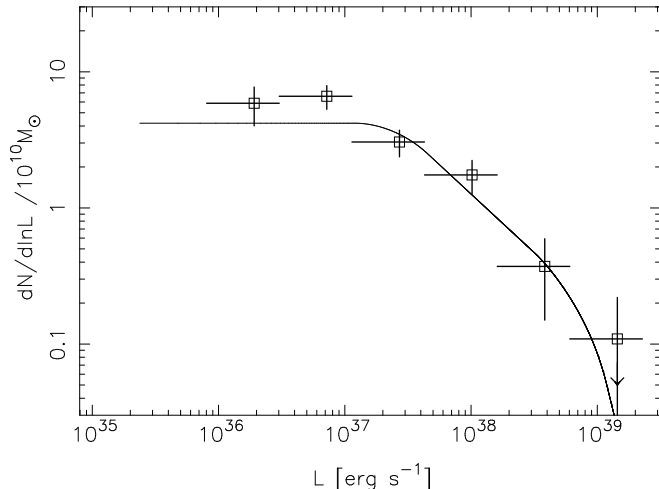


FIG. 5.— The LF of low-mass X-ray binaries within 5 arcmin from the center of Cen A, normalized to the stellar mass including GC sources. The contribution of resolved background sources has been subtracted using the CXB source counts of Moretti et al. (2003) with normalization increased by a factor of 1.5, as described in the text. The luminosity function is corrected for incompleteness. The solid line is the average LF of LMXBs in nearby galaxies (Gilfanov 2004).

LMXBs is constructed using the following prescription:

$$\frac{dN_{xrb}}{dL} = \frac{1}{f_{xrb}(L)} \left(\frac{dN_o}{dL} - \frac{f_b(L)}{4\pi D^2} \frac{dN_b}{dS} \right) \quad (1)$$

where dN_o/dL is the raw observed LF of all sources, $f_{xrb}(L)$ and $f_b(L)$ are the incompleteness functions for X-ray binaries and CXB sources, dN_b/dS is the predicted $\log(N) - \log(S)$ distribution for CXB sources, and D is the distance to Cen A. The raw observed LF distribution is constructed down to the luminosity limit L_{min} at which the incompleteness equals $f_{xrb}(L_{min}) = 0.5$. This sets up the limiting luminosity to which the final LF is constructed. The luminosity limit varies somewhat, but not dramatically, depending on the region being analyzed and the assumed source distribution, from $L_{min} \approx 7.0 \times 10^{35}$ erg s $^{-1}$ for field LMXBs within 2.5 arcmin from the center of Cen A, to $L_{min} \sim 10^{36}$ erg s $^{-1}$ for background sources in the 5.0 – 7.5 annulus. Further out the incompleteness quickly becomes severe, with the 0.5 completeness limit being at $L_{min} \sim 3 \times 10^{36}$ erg s $^{-1}$ in 7.5 – 10.0 arcmin annulus (from which only GC LMXBs are included in the present study, as the number of field LMXBs are negligible in this region). The incompleteness functions for the GC and field source samples are shown in Fig. 4. In the inner parts the main factor limiting the sensitivity is the strong diffuse emission, whereas further out it is the increased size of the PSF, and the fact that not all regions are covered by all of the observations. The most sensitive region is therefore at distances of about 2 arcmin from the centre, where sources can be detected down to $\sim 5 \times 10^{36}$ erg s $^{-1}$.

4. RESULTS

In Fig. 5 the LF of all the LMXBs within a radius of 5 arcmin is shown. It is obvious from this figure that at luminosities above $\sim 10^{37}$ erg s $^{-1}$ the LF is consistent with a power law with the slope $\Gamma \sim 1.8 - 2.0$, found in previous studies of populations of compact sources in early type galaxies Gilfanov (2004); Kim & Fabbiano (2004).

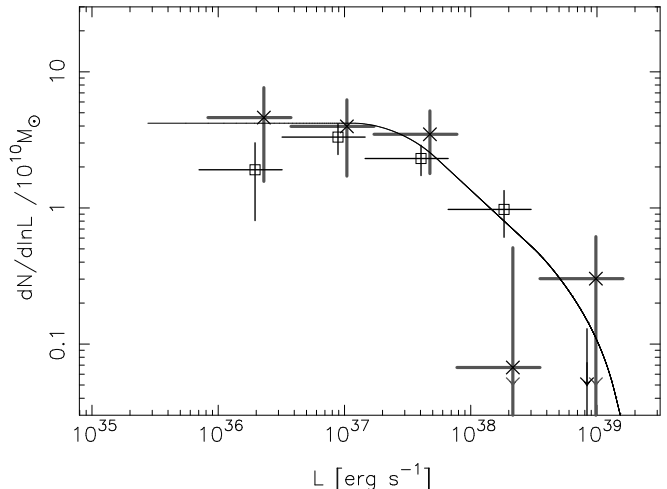


FIG. 6.— The LF of X-ray binaries in the inner 0.0 – 2.5 arcmin (open squares) and 2.5 – 7.5 arcmin (crosses) annulus. The latter region extends outside the 5.0 arcmin used for analysing field sources in the rest of this paper, to maximally probe radial differences. Although the background and incompleteness corrections differ strongly in the two regions, the final luminosity distributions are consistent with each other.

It becomes nearly flat in $dN/d(\ln L)$ units below this luminosity, also in agreement with the behavior found earlier, namely in the Milky Way, bulge of M31 and in the Cen A galaxy itself, but based on a much smaller dataset (Gilfanov 2004; Voss & Gilfanov 2006, 2007a).

We applied various statistical tests to perform a more quantitative comparison with the results of previous studies. First we tested if the data are consistent with a single power law using the Kolmogorov-Smirnov (KS) test. We find that a power-law slope of $\Gamma = 1.8$ is unacceptable with a probability of $5 \cdot 10^{-7}$, whereas more shallow slopes in the range 1.3-1.4 are acceptable with the K-S probability of $\gtrsim 10\%$. The broken power-law fit to the data with all parameters free does not give constraining results, mainly due to insufficient statistics of the LF in the bright end. On the other hand, the high luminosity slope of the LMXB LF is rather well constrained based on the data for more massive (and more distant) elliptical galaxies (Gilfanov 2004; Kim & Fabbiano 2004). We therefore fix the high luminosity index at $\Gamma = 1.8$ and fit the data, leaving the break luminosity and the power-law index of LF below the break free parameters of the fit. The best fit values of these parameters are: $L_b = (3.9^{+1.6}_{-2.3}) \cdot 10^{37}$ erg/s and $\Gamma_2 = 1.2 \pm 0.1$. A model with the low luminosity index fixed at $\Gamma_2 = 1$ is also consistent with the data with a KS probability of 67%¹⁹, resulting in a best fit value of the break luminosity $L_b = (1.7 \pm 0.7) \cdot 10^{37}$ erg/s. These numbers are consistent with the parameters from Gilfanov (2004). However, they are lower than the value of $5.0^{+1.0}_{-0.7} \cdot 10^{37}$ erg s $^{-1}$ found by Voss & Gilfanov (2006). That study was based on shallower data, for which it was not possible to reliably exclude source contamination from the extended emission, and therefore the results of our study are much more reliable, even if the deeper data do not improve the

¹⁹ We note that this is not consistent with the errors on the low luminosity slope found from the maximum likelihood fit. This is possible because the two tests used to find the best fit and the goodness of the fit are independent (unlike the χ^2 test).

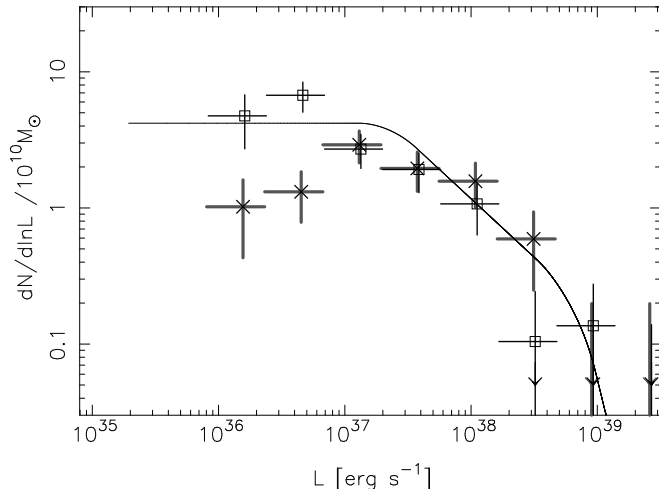


FIG. 7.— LFs of the field (non-GC, squares) and GC (crosses, arbitrary normalization) samples. The contribution of background sources was subtracted and incompleteness correction was applied. The relative paucity of faint sources in the LF of GC sources is apparent. The two distributions are different at the $\approx 3.4\sigma$ level. Note that although there are more sources in the field sample, the errors are comparable to the GC sample, due to the (subtracted) contribution of CXB sources.

statistics dramatically.

We also compare the luminosity distribution in the central $0.0 - 2.5$ arcmin to the distribution in the $2.5 - 7.5$ arcmin annulus. As these two regions are subject to different systematic effects, a comparison between them can be used to assess the accuracy of our analysis. Near the center diffuse gas and variable absorption are primary factors, while the background subtraction is unimportant. In the outer region the background subtraction is the most important effect. Fig. 6 demonstrates that LFs for these two regions are consistent with each other within statistical errors.

4.1. Globular cluster and field sources

Fig. 7 compares the LFs of the GC and field ($0.0 - 5.0$ arcmin) samples. The two distributions appear to be different, with the LF of the GC sample having a pronounced deficit of faint sources, $\log(L_X) \lesssim 36.5$. The difference in corrections (background subtraction and incompleteness corrections) makes the use of the KS-test for statistical comparison of the two distributions non-trivial. For this reason, we chose to employ a simpler test, in which we compare ratios of faint to bright sources, $R = N_{faint}/N_{bright}$. We define faint and bright sources as those in the luminosity range from 10^{36} to 10^{37} erg s^{-1} and above 10^{37} erg s^{-1} respectively. The boundary was chosen rather arbitrarily, motivated by the shape of the luminosity function and the requirement to optimize the numbers of sources in both bins for both samples in order to be sensitive to differences in the LFs. The final result is not particularly sensitive to the precise value of this boundary.

The computed faint-to-bright ratios for the field and GC samples are presented in Table 2, where they are compared to the field and spectroscopically confirmed GCs LMXBs in M31 from the study of Voss & Gilfanov (2007a). Because of the non-Gaussianity of errors in the ratio R , caused by the small numbers of sources, we use Monte Carlo simulations to assess the errors and

significances of our results. In each Monte-Carlo run we recompute the number of sources in each luminosity bin. For each observed source a random number is drawn from a Poisson distribution with an expectation value of 1, and the same corrections are applied to the obtained Monte-Carlo sample as the ones used to correct the observed sample. These numbers are then summed, giving the N_{faint} and N_{bright} of the Monte Carlo realization from which the value of R is computed. The dispersion of the latter is used to estimate the uncertainty in R , cited in Table 2. The statistical significance of two LFs being different is estimated based on the null hypothesis $R_F - R_{GC} = 0$, which is calculated from the fraction of 10^6 Monte Carlo realizations in which $R_F - R_{GC} > 0$. From these calculations we find $R_{GC} = 0.56^{+0.20}_{-0.16}$, which is well below the value for the field sample, $R_F = 2.50^{+0.82}_{-0.62}$. The statistical significance of the difference between the two distributions is 99.97% which corresponds to 3.4σ . As an additional check, we repeated the above analysis with the cleanest sample possible, entirely excluding the regions marked by boxes in Fig. 1, in addition to the jet and nucleus region. With this reduced sample, we still find that the field and GC distributions are different at the 99.89% confidence level ($\approx 3.1\sigma$). We are therefore confident that the population of LMXBs in GCs is different from the field population, with a relative underabundance of faint sources in the GCs, and that this result is not caused by contamination of our sample by spurious sources from the regions with strong diffuse emission.

5. DISCUSSION

5.1. Field sources

The luminosity function of low-mass X-ray binaries in old stellar environments is fairly well studied in the bright source limit, $\log(L_X) \gtrsim 37.5$, where it was shown to follow a rather steep power law with slope $\Gamma \approx 1.8 - 1.9$ (Gilfanov 2004; Kim & Fabbiano 2004). It steepens further above the Eddington limit for a neutron star, $\log(L_X) \gtrsim 38.5 - 38.6$, and no LMXBs significantly more luminous than $\log(L_X) \sim 39.5$ appear to exist. This behavior seems to be universal for compact X-ray sources associated with old stellar populations. With a large number of spiral and elliptical galaxies extensively studied by different groups of researchers, no significant deviations from this behavior have been identified. Due to obvious restrictions resulting from the sensitivity of a typical *Chandra* observation, the faint end of the luminosity function of point sources has not been studied as extensively as the bright end, and so a consensus has not emerged.

With the currently available *Chandra* data it is possible to study the LF of compact sources well below 10^{37} erg s^{-1} only in a handful of sufficiently large and nearby galaxies; M31, Cen A and NGC3379 being the most significant among them. The LMXB LF is also known for the Milky Way. It has been found that LMXB LFs in the Milky Way and M31 show consistent behavior, with a clear low-luminosity break at $\log(L_X) \sim 37.5$ below which they follow a $dN/dL \propto L^{-1}$ power law (Gilfanov 2004; Voss & Gilfanov 2007a). Above the break, the LF shape is similar to that of compact sources in elliptical galaxies. In a previous study of Cen A, based on ~ 200

ks of exposure, it was shown that the LF of compact sources there also exhibits a break at a few times 10^{37} erg s⁻¹ (Voss & Gilfanov 2006). However, the statistical quality of the data did not permit an accurate constraint of the position of the break and the slope of the luminosity distribution. The study of two other nearby early-type galaxies gave results to the contrary, claiming that the $\Gamma \approx 1.8$ power law continues below $\log(L_X) \sim 37$ (Kim et al. 2006). It should be mentioned that the latter result was based on a more shallow dataset than the one in which the break was found. It remained unclear whether this discrepancy is caused by the statistical effects and/or systematic differences in the data treatment (in particular, correction for the sample incompleteness) or, on the contrary, demonstrates that properties of the LMXB population may differ between the early and late type galaxies and even between early-type galaxies with different star-formation history. The latter possibility would not be entirely unexpected, because the population of LMXBs does evolve on \sim Gyr timescales.

With the data of the very deep VLP program of Cen A observations we have demonstrated with high confidence the presence of the low luminosity break in the LF of compact sources in this galaxy. Its overall qualitative behavior and particular values of the best fit parameters agree well with the results for the Milky Way and M31.

Although a complete theoretical description of the LMXB LF is yet to be created, a plausible scenario has been sketched by Postnov & Kuranov (2005) (see also Bildsten & Deloye (2004)). They suggested that the break in the luminosity distribution of LMXBs corresponds to the transition from binary systems, in which the mass transfer is driven by magnetic braking of the secondary, to the binary systems losing orbital angular momentum through the emission of gravitational waves. In this interpretation the low luminosity part of the population obeying the $dN/dL \propto L^{-1}$ law is dominated by short orbital period binaries with very low mass donors, $M_d \lesssim 0.4M_\odot$. This prediction allows, in principle, direct observational proof through study of the properties of individual binaries in the Milky Way and nearby galaxies. While this is yet to be done, the reliable determination of the LMXB shape and accurate measurements of its parameters provided by observations mentioned above and reported in this paper lend indirect support to this scenario.

5.2. Globular cluster sources

The difference between luminosity distributions of primordial and dynamically formed binaries was first suggested by Voss & Gilfanov (2007a) based on the analysis of LFs of LMXBs in the field, in GCs and in the nucleus of M31. To obtain a statistically significant result they had to combine GC sources with LMXBs in the nucleus of M31, also shown to be formed dynamically in close stellar encounters (Voss & Gilfanov 2007b). Studies of populations of compact sources in NGC 3379 (Fabbiano et al. 2007), NGC 4278 and NGC4697 (Kim et al. 2009) also find a relative dearth of low luminosity LMXBs in GCs, even if it is only possible to probe the LFs to a limit of $\sim 5 \times 10^{36}$ erg s⁻¹ in these galaxies. Also analysis of early Cen A data (Woodley et al. 2008) indicate a relative dearth of low luminosity LMXBs in globular clusters. However, the latter analysis yielded results of low

statistical significance, and, more importantly, ignored the issue of background source contribution. The slope of the CXB $\log N - \log S$ is $\Gamma \sim 1.4 - 1.6$ in the flux range of interest (Moretti et al. 2003). As this is steeper than the LF of the field LMXBs, to neglect their contribution may lead to artificially high confidence estimates. Furthermore, the study of Woodley et al. (2008) did not take incompleteness effects into account, and they concluded that it was not clear if their analysis was not compromised by the sample incompleteness. The results presented above are therefore the most robust and statistically significant evidence yet for a difference between the luminosity distributions of LMXBs in the field and in globular clusters.

Taken at face value, the observed difference between LFs suggests that LMXBs in the field and in globular clusters belong to two different populations. This may finally falsify the hypothesis that all LMXBs in galaxies are formed in globular clusters (as first suggested by White et al. 2002).

It is not likely that any further significant improvement in the statistical quality of the LFs and confidence level of this result can be achieved with yet longer observations of the Cen A galaxy, or, in general, with other observations of individual galaxies. The observed fall-off of the GC XLF at low luminosities indicates that we are picking up the majority of the globular cluster LMXBs and no significant further increase in their numbers should be expected. On the other hand, due to the L^{-1} behavior of the luminosity distribution, the sample of field LMXBs is increasing only logarithmically with flux. Moreover, the faint end of the source sample will become increasingly polluted with the background sources, for which the flux distribution is steeper, and the increased source density may lead to increased confusion effects, especially in the inner region of the galaxy, which will further compromise the sample of faint sources. A more realistic way to obtain high-quality XLF of the dynamically formed sources suitable for a meaningful analysis is to combine data for a number of nearby galaxies, for which *Chandra* data have a sufficiently low sensitivity threshold. The same is true with respect to the luminosity function of the field sources.

5.3. Interpretation

The disproportionately (with respect to the stellar mass) large number of X-ray binaries found in globular clusters can be explained by the formation of binaries in close stellar encounters (Clark 1975). The following three processes are believed to be the main channels of dynamical formation of X-ray binaries in high stellar density environments typical of globular clusters: (i) a tidal capture of a neutron star (NS) by a non-degenerate single star (Fabian et al. 1975), (ii) a collision of a NS with an evolved star on the subgiant or red giant branch (RGB) (Verbunt 1987) and (iii) an exchange reaction, in which a NS exchanges place with a star in a pre-existing binary during a close binary-single encounter (Hills 1976). With the possible exception of collisions with evolved stars which may lead to formation of an ultra-compact binary, it is difficult or impossible to observationally distinguish between the products of these processes, and it is therefore difficult to determine their relative contributions to the populations of X-ray binaries in GCs. The-

oretical estimates show that they may be making comparable contributions (Voss & Gilfanov 2007b), but the numbers may also depend on GC parameters (see e.g. Ivanova et al. 2008).

Collisions between neutron stars and red (sub-) giants can lead to the formation of an X-ray binary, in which the donor star is a white/brown dwarf or a helium star, depending on the evolutionary stage of the evolved star before the collision (Ivanova et al. 2005). This may offer a plausible explanation for the observed deficit of faint sources in GCs. As the donor star has lost all of its hydrogen envelope in the course of the common envelope phase, the material in the accretion disk will be He-rich. Because of the 4 times higher ionization potential of He, the accretion disk instability will appear at higher \dot{M} value than in the case of an accretion disk of solar composition. Quantitatively, the critical accretion rate value \dot{M}_{crit} is ~ 20 times larger for a pure He disk than for a disk composed of solar abundance material (Lasota et al. 2008). The theoretical lower limit on the bolometric luminosity of persistent systems with orbital period of $P_{\text{orb}} = 60$ min (approximately the shortest period possible for non-degenerate donor stars) changes from $\sim 10^{36}$ erg/s for a solar abundance disk to $\sim 2 \cdot 10^{37}$ erg/s for a pure He disk (Lasota et al. 2008, assuming accretion efficiency of 0.2). It is smaller for more compact systems, decreasing as $P_{\text{orb}}^{\approx 1.6-1.7}$. We note that due to the limited energy range covered by *Chandra*, the observational luminosities are somewhat smaller than the theoretical estimates, and corrections due to this suffer from relatively large spectral uncertainties.

The majority of field (non-GC) LMXBs are likely to have main sequence donors, unless they are formed in globular clusters. This is expected theoretically in the models of primordial binary evolution and is also confirmed by the statistics of X-ray binaries in the Milky Way (Liu et al. 2007). If a significant fraction of X-ray binaries in globular clusters have He donors, this may explain the smaller fraction of low luminosity systems as compared with the field population, as they will not be observed as persistent sources below the transience limit L_{crit} . In this scenario not only is the number of faint sources reduced, but also the number of luminous ones is possibly increased due to intrinsically faint systems that are currently in outburst. Calculations of the luminosity distribution of X-ray binaries accounting for these effects appear to be beyond the predictive power of the current generation of population synthesis codes. The problem is further complicated by the fact that the accurate calculation of the formation rates of various types of binaries is insufficient, as evolution, X-ray lifetimes and transient behavior of the binaries should also be considered. Estimates of Voss & Gilfanov (2007b) indicate that He-accreting systems may contribute about $\sim 1/3$ to the LMXB population of globular clusters, in rough agreement with the statistics of globular cluster sources in the Milky Way. This may be sufficient to explain the fall-off of the GC LF to low luminosities, although modelling would depend on the details of the luminosity distribution of X-ray binaries formed via other formation mechanisms (which may differ from the LF of field sources) and on the fraction of He-accreting systems in outburst. On the other hand, the fact that the value of

the critical luminosity limit for persistent He-accreting systems, $\sim 10^{37}$ erg/s, is in the range where the GC LF fall-off begins, gives an indirect support to the proposed scenario. A more direct observational test may come from statistics of transient sources in globular clusters in nearby galaxies.

6. CONCLUSIONS

We have studied the luminosity function of LMXBs in the early-type galaxy Centaurus A (NGC 5128), with particular emphasis on its behavior in the low luminosity regime and special attention to various systematic and instrumental effects that may compromise the faint end of the luminosity distribution of compact sources in such a complicated galaxy. We demonstrated that substructures in the diffuse emission can significantly pollute the source list produced by the automated point source detection software. This effect, less obvious with previous shorter observations, became especially evident with the deep ~ 800 ks exposure collected by the *Chandra* VLP program for this galaxy. We also performed accurate corrections for incompleteness and removal of the contribution of resolved background sources.

We confirm with high statistical confidence that the luminosity function of the LMXBs flattens significantly below $\log(L) \sim 37.5$ and is inconsistent with extrapolation of the $\Gamma \approx 1.8$ power law observed in numerous elliptical galaxies at higher luminosities. In the low luminosity regime it is consistent with the logarithmically flat distribution predicted by some theories of binary evolution and previously observed in two other nearby galaxies.

We find with a confidence of 99.97% that the luminosity distribution of LMXBs in globular clusters differs from that of the field (non-globular cluster) LMXBs, with a relative lack of low-luminosity sources in the globular cluster sample. This may finally falsify the hypothesis that the entire population of LMXBs in early type galaxies has been formed in globular clusters. As a plausible explanation for this difference we suggest that there is a large fraction of binaries with He-rich donors in the LMXB population in globular clusters. These systems will show transient behavior at ~ 20 times higher accretion rate than X-ray binaries with a normal main sequence donor and therefore would not be detected among persistent sources with $\log(L_X) \lesssim 37.0 - 37.5$. In globular clusters, they may be created in sufficient numbers in collisions of compact objects with red (sub-) giants, whereas their number among the field sources is small. An observational check for this scenario may come from statistics of transient sources in globular clusters.

This research has made use of data obtained from the *Chandra* Data Archive and software provided by the *Chandra* X-ray Center (CXC) in the application package CIAO. This work was supported by the NASA grants GO7-8105X and NAS8-03060. R.V. acknowledges the support by the DFG cluster of excellence 'Origin and Structure of the Universe' (<http://www.universe-cluster.de>). CLS and GRS were supported in part by Hubble Grants HST-GO-10597.03-A, HST-GO-10582.02-A, and HST-GO-10835.01-A, and Chandra Grant GO8-9085X. MSH thanks the Royal Society for support. The authors would like to thank the

anonymous referee for constructive criticism of the original manuscript which helped to improve the paper.

Facilities: Chandra (ACIS).

REFERENCES

- Bell, E., & De Jong, R. 2001, *ApJ*, 550, 212
 Bildsten, L., & Deloye, C.J. 2004, *ApJ*, 607, L119
 Cappelluti, N. et al. 2005, *A&A*, 430, 39
 Clark, G. W. 1975, *ApJ*, 199, L143
 Croston, J.H., 2009, *MNRAS*, 395, 1999
 Dickey, J.M., & Lockman, F.J. 1990, *ARA&A*, 28, 215
 Dufour, R.J., et al. 1979, *AJ*, 84, 284
 Evans, D.A. et al. 2004, *ApJ*, 612, 786
 Fabbiano, G. et al. 2007, arXiv:astro-ph/0710.5126
 Fabian, A. C., Pringle, J. E., & Rees, M. J. 1975, *MNRAS*, 172, 15
 Ferrarese, L., Mould, J.R., Stetson, P.B., Tonry, J.L., Blakeslee, J.P. & Ajhar, E.A. 2007, *ApJ*, 654, 186
 Gilfanov, M. 2004, *MNRAS*, 349, 146
 Grimm, H.-J., Gilfanov, M.R., & Sunyaev, R.A. 2003, *MNRAS*, 339, 793
 Hardcastle, M.J. et al. 2003, *ApJ*, 593, 169
 Hardcastle, M.J., et al. 2007, *ApJ*, 670, L81
 Harris, G. L. H., et al. 2004, *AJ*, 128, 712
 Hills, J. G. 1976, *MNRAS*, 175, 1
 Hudaverdi, M., Kunieda, H., Tanaka, T., Haba, Y., Furuzawa, A., Tawara, Y., & Nihal Ercan, E. 2008, arXiv:astro-ph/0803.2575
 Humphrey, P.J., & Buote, D.A., 2008, *ApJ*, 689, 983
 Illarionov, A. F., & Sunyaev, R. A. 1975, *A&A*, 39, 185
 Irwin, J.A. 2005, *ApJ*, 631, 511
 Ivanova, N., Rasio, F. A., Lombardi, J. C., Dooley, K. L., & Proulx, Z. F. 2005, *ApJ*, 621, L109
 Ivanova, N., Heinke, C.O., Rasio, F.A., Belczynski, K., & Fregeau, J.M. 2008, *MNRAS*, 386, 553
 Jarret, T.H., Chester, T., Cutri, R., Schneider, S., & Huchra, J.P. 2003, *AJ*, 125, 525
 Jordán et al. 2004, *ApJ*, 613, 279
 Jordán et al. 2007, *ApJ*, 671, L117
 Jordán et al. 2008, in preparation
 Juett, A.M. 2005, *ApJ*, 621, 25
 Karovska, M. et al. 2002, *ApJ*, 577, 114
 Kim, D.-W., & Fabbiano, G. 2004, *ApJ*, 613, 933
 Kim, D.-W. et al. 2006, *ApJ*, 652, 1090
 Kim, D.-W., et al., 2009, arXiv:astro-ph/0902.2343
 Kraft, R.P., Kregenow, J.M., Forman, W.R., Jones, C., & Murray, S.S. 2001, *ApJ*, 560, 675
 Kraft, R.P. et al. 2002, *ApJ*, 569, 54
 Kraft, R.P. et al. 2003, *ApJ*, 592, 129
 Kraft, R.P. et al. 2007, *ApJ*, 665, 1129
 Kraft, R.P. et al. 2007, *ApJ*, 677, 97
 Kundu, A., Maccarone, T.J., & Zepf, S.E. 2002, *ApJ*, 574, 5
 Kundu, A., Maccarone, T.J., & Zepf, S.E. 2007, *ApJ*, 662, 525
 Lasota, J.-P., Dubus, G. & Kruk, K., 2008, *A&A*, 486, 523
 Liu, Q.Z., van Paradijs, J., & van den Heuvel, E.P.J. 2007, *A&A*, 469, 807
 Maccarone, T.J., Kundu, A., & Zepf, S.E. 2003, *ApJ*, 586, 814
 Minniti, D., Rejkuba, M., Funes, J.G., & Akiyama, S. 2004, *ApJ*, 600, 716
 Moretti, A., Campana, S., Lazzati, D., & Tagliaferri, G. 2003, *ApJ*, 588, 696
 Peng, E. W., Ford, H. C., & Freeman, K. C. 2004, *ApJS*, 150, 367
 Posson-Brown, J., Raychaudhury, S., Forman, W., Donnelly, R.H., Jones, C., 2009, *ApJ*, 695, 1094
 Postnov, K.A., & Kuranov, A.G. 2005, *Astro. Lett.*, 31, 7
 Raychaudhury, S. 1989, *Nature*, 342, 251
 Sarazin, C., Irwin, J.A., & Bregman, J.N. 2000, *ApJ*, 544, L101
 Sarazin, C.L., Kundu, A., Irwin, J.A., Sivakoff, G.R., Blanton, E.L., & Randall, S.W. 2003, *ApJ*, 595, 743
 Shtykovskiy, P., & Gilfanov, M. 2005, *MNRAS*, 362, 879
 Sivakoff, G.R., et al. 2007, *ApJ*, 660, 1246
 Sivakoff, G.R., et al. 2008a, *ApJ*, 677, 27
 Verbunt F. 1987, *ApJ*, 312, L23
 Voss, R., & Gilfanov, M. 2006, *A&A*, 447, 71
 Voss, R., & Gilfanov, M. 2007a, *A&A*, 468, 49
 Voss, R., & Gilfanov, M. 2007b, *MNRAS*, 380, 1685
 White, R.E., III, Sarazin, C.L., & Kulkarni, S.R. 2002, *ApJ*, 571, 23
 Woodley, K.A., Harris, W.E., Beasley, M.A., Peng, E.W., Bridges, T.J., Forbes, D.A., & Harris, G.L.H. 2007, *AJ*, 134, 494
 Woodley, K.A. et al. 2008, *ApJ*, 682, 199
 Worrall, D.M., et al. 2008, *ApJ*, 673, L135

TABLE 1
THE *Chandra* OBSERVATIONS USED IN THIS PAPER.

Obs-ID	Date	Instrument	Exp. Time	R.A.	Dec.	Data Mode
0316	1999 Dec 05	ACIS-I	36.18 ks	13 25 27.61	-43 01 08.90	FAINT
0962	2000 May 17	ACIS-I	36.97 ks	13 25 27.61	-43 01 08.90	FAINT
2987	2002 Sep 03	ACIS-S	45.18 ks	13 25 28.69	-43 00 59.70	FAINT
3965	2003 Sep 14	ACIS-S	50.17 ks	13 25 28.70	-43 00 59.70	FAINT
7797	2007 Mar 22	ACIS-I	98.17 ks	13 25 19.15	-43 02 42.40	FAINT
7798	2007 Mar 27	ACIS-I	92.04 ks	13 25 51.80	-43 00 04.43	FAINT
7799	2007 Mar 30	ACIS-I	96.04 ks	13 25 51.80	-43 00 04.43	FAINT
7800	2007 Apr 17	ACIS-I	92.05 ks	13 25 46.00	-42 58 14.58	FAINT
8489	2007 May 08	ACIS-I	95.18 ks	13 25 32.79	-43 01 35.13	FAINT
8490	2007 May 30	ACIS-I	95.68 ks	13 25 18.79	-43 03 01.72	FAINT

TABLE 2
THE RATIOS OF FAINT TO BRIGHT SOURCES IN CEN A AND M 31.

Region	N_{faint}^a	N_{bright}^a	B_{faint}^b	B_{bright}^b	$N_{cor,faint}^c$	$N_{cor,bright}^c$	Ratio
GCs	17	30	0.9	0.4	16.7	29.6	$0.56^{+0.20}_{-0.16}$
Field	96	50	43.0	14.6	88.5	35.4	$2.50^{+0.82}_{-0.62}$
M 31 GC	3	8	0	0	3	8	$0.38^{+0.34}_{-0.24}$
M 31 field	40	19	15.5	0.8	24.6	18.2	$1.35^{+0.58}_{-0.42}$

NOTE. — The subscripts *faint* and *bright* corresponds to sources in the $10^{36} - 10^{37}$ erg s⁻¹ and $> 10^{37}$ erg s⁻¹ ranges, respectively.

^a Observed uncorrected number of sources.

^b Expected number of background sources.

^c Background subtracted and incompleteness corrected number of sources (including correction for the change in survey area below 5×10^{36} erg s⁻¹ due to the exclusion of problematic regions).